PHYSICAL REVIEW B **75**, 245106 (2007)

Infrared study on the electronic structure of the alkaline-earth-filled skutterudites AM_4Sb_{12} (A=Sr, Ba; M=Fe, Ru, Os)

Shin-ichi Kimura,[1,2,*] Hojun Im,[2,†] Takafumi Mizuno,[2] Shota Narazu,[3] Eiichi Matsuoka,[3,‡] and Toshiro Takabatake[3,4]
[1]*UVSOR Facility, Institute for Molecular Science, Okazaki 444-8585, Japan*
[2]*School of Physical Sciences, The Graduate University for Advanced Studies (SOKENDAI), Okazaki 444-8585, Japan*
[3]*Department of Quantum Matter, ADSM, Hiroshima University, Higashi-Hiroshima 739-8530, Japan*
[4]*Institute for Advanced Materials Research, Hiroshima University, Higashi-Hiroshima 739-8530, Japan*

(Received 5 February 2007; revised manuscript received 28 March 2007; published 11 June 2007)

The optical conductivity [$\sigma(\omega)$] spectra of alkaline-earth-filled skutterudites with the chemical formula $A^{2+}M_4Sb_{12}$ (A=Sr, Ba; M=Fe, Ru, Os) and a reference material $La^{3+}Fe_4Sb_{12}$ were obtained and compared with the corresponding band-structure calculations and with calculated $\sigma(\omega)$ spectra to investigate their electronic structures. At high temperatures, the energy of the plasma edge decreased with the increasing valence of the guest atoms A in the Fe_4Sb_{12} cage indicating hole-type conduction. A narrow peak at 25 meV with a pseudogap was observed in $SrFe_4Sb_{12}$, while the corresponding peaks were located at 200 and 100 meV in the Ru and Os counterparts, respectively. The order of the peak energy in these compounds is consistent with the thermodynamical properties in which the Os compound is located between the Fe and Ru compounds. This indicated that the electronic structure observed in the infrared $\sigma(\omega)$ spectra directly affects the thermodynamical properties. The band-structure calculation implies that the different electronic structures among these compounds originate from the different d states of the M ions.

DOI: 10.1103/PhysRevB.75.245106 PACS number(s): 78.30.−j, 71.20.Lp, 75.50.Bb

I. INTRODUCTION

Rare-earth-filled skutterudites have recently attracted attention due to their various unique physical properties such as the magnetic-field-induced quadrupole order in $PrOs_4Sb_{12}$,[1] the pressure-induced superconducting phase in $PrRu_4P_{12}$,[2] new ordered states in high magnetic fields in $PrFe_4P_{12}$,[3] a multipole ordered state in $SmRu_4P_{12}$,[4] and the magnetic-field-independent heavy fermion state in $SmOs_4Sb_{12}$ (Ref. 5) to name a few. These unconventional physical properties indicate that the combination of the guest rare-earth ions and the other two elements of the cage produces unique physical environments due to the strong hybridization between these ions. In the filled-skutterudite case, the crystal structure shown in Fig. 1 [body-centered-cubic structure with $Im\bar{3}$ (T_h^5) (Ref. 6)], AM_4X_{12} (A, guest atom; M, transition metals; X, pnictogen), is the key for this strong hybridization. The crystal structure makes nanosized cages composed of M_4X_{12}. The guest atoms A are located in these cages.[7] The strong hybridization between the A ion and the M_4X_{12} cage is believed to be the origin of the various unique physical properties mentioned above. In addition, the electronic structure of the M_4X_{12} frame is also important in determining the bulk physical properties, particularly given the magnetic moment of the M ion. For example, in the case of nonmagnetic guest atoms, alkali-metal-filled iron antimony skutterudites (KFe_4Sb_{12} and $NaFe_4Sb_{12}$) exhibit weak itinerant ferromagnetism due to the Fe 3d electrons.[8–10] These skutterudites also produce iron-based heavy quasiparticles as a result.[11,12]

In the filled-skutterudite compounds, the positional parameters u and v of the Sb atoms defined in Fig. 1 are also important in determining the physical properties as well as the electronic structure.[13] These parameters change depending on the different A and M atoms. Given the positional dependence, it is important to ascertain the relationship between these parameters and the electronic structure as well as the physical properties.

Alkaline-earth-filled antimony skutterudites AM_4Sb_{12} (A=Ca, Sr, Ba; M=Fe, Ru, Os) have been vigorously investigated.[14] Among these materials, AFe_4Sb_{12} materials have an electrical resistivity with a shoulder at 70 K with a quadratic dependence upon decreasing temperatures, a thermopower with a local maximum at around 50 K, an electronic specific-heat coefficient γ of 100 mJ/mol K^2, and a maximum magnetic susceptibility at 50 K, which commonly implies the presence of low-energy spin fluctuations described by the self-consistent renormalization (SCR) theory.[15,16] The ratio between the enhanced coefficient A of the quadratic electrical resistivity ($\rho=AT^2$) and γ is close to the Kadowaki-Woods value [1.0×10^{-5} $\mu\Omega$ cm K^{-2}/(mJ/mol K^2)^2]. This phenomenon originates from the presence of heavy quasiparticles, ob-

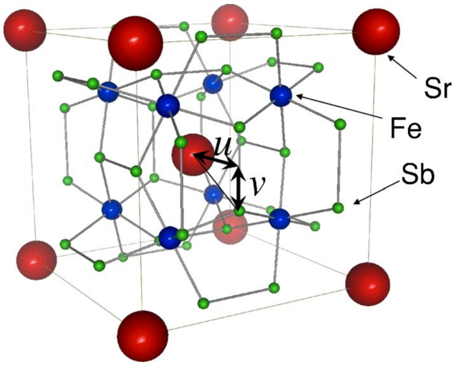

FIG. 1. (Color online) The crystal structure of $SrFe_4Sb_{12}$. The unit cell is marked by lines. The positional parameters u and v of an Sb atom are denoted.

served in an infrared reflectivity experiment, arising from the Fe 3*d* electrons.[12] In comparison, alkaline-earth-filled ruthenium antimony skutterudites, $A^{2+}Ru_4Sb_{12}$, exhibit normal metallic physical properties with a small electrical specific-heat coefficient, $\gamma=10$ mJ/mol K^2. The electrical resistivities of $A^{2+}Os_4Sb_{12}$ compounds exhibit a pronounced shoulder at 100 K, a magnetic susceptibility with a logarithmic temperature dependence, and a moderately high γ value of 45 mJ/mol K^2.[17] The thermodynamical properties of the Os compounds imply that they are located between the Fe and Ru compounds.

To clarify the differences in the physical properties in $A^{2+}M_4Sb_{12}$ compounds (A=Sr, Ba; M=Fe, Ru, Os), the optical conductivity $[\sigma(\omega)]$ spectra of these compounds were obtained and compared with the band-structure calculations. The specific purpose of this comparison is to observe the differences between the experimental and calculated $\sigma(\omega)$ spectra using the lattice constants and the positional parameters experimentally obtained by x-ray diffraction. To check the effects of the change of the positional parameters of the Sb atoms, the band structures of $SrFe_4Sb_{12}$ were also calculated using the positional parameters of the Ru counterpart. In the next section, the experimental and analytical methods including the theoretical calculations are explained. In Sec. III, the experimental and the calculated $\sigma(\omega)$ spectra are compared and which parameter is more influential regarding the electronic structure near the Fermi level (E_F) is discussed. The results are summarized in Sec. IV.

II. EXPERIMENTAL AND BAND CALCULATION METHODS

High-density polycrystalline AM_4Sb_{12} samples were synthesized using a spark-plasma sintering technique previously reported.[15] The near-normal incident optical reflectivity $[R(\omega)]$ spectra were acquired from well-polished samples by using 0.3 μm grain-size Al_2O_3 wrapping film sheets. Martin-Puplett- and Michelson-type rapid-scan Fourier spectrometers (JASCO Co. Ltd., FARIS-1 and FTIR610) were used at photon energies ($\hbar\omega$) of 2.5–30 meV and 5 meV–1.5 eV, respectively, at sample temperatures in the range of 7–300 K using a closed cycle helium cryostat for FTIR610 and a liquid-helium flow-type cryostat for FARIS-1. To obtain the absolute $R(\omega)$ values, the samples were evaporated *in situ* with gold, whose spectrum was then measured as a reference. To obtain $\sigma(\omega)$ spectra via the Kramers-Kronig analysis (KKA), $R(\omega)$ was measured at 300 K over the energy range of 1.5–30 eV at the synchrotron radiation beamline 7B of UVSOR-II, at the Institute for Molecular Science.[18] Since $R(\omega)$ does not significantly change with temperature above 1.5 eV, the $R(\omega)$ spectra above 1.5 eV were connected to the $R(\omega)$ spectra at other temperatures in the energy range below 1.5 eV. In the energy ranges below 2.5 meV and above 30 eV, the spectra were extrapolated using the Hagen-Rubens function $[R(\omega)=1-(2\omega/\pi\sigma_{dc})^{1/2}]$ and the $R(\omega) \propto \omega^{-4}$ relationship, respectively.[19] Here, σ_{dc} denotes the direct current conductivity. After constructing $R(\omega)$ in the energy region from zero to infinity, the KKA was performed to obtain the $\sigma(\omega)$ spectrum.

TABLE I. The lattice constants and the positional parameters (u,v) of Sb atoms in AM_4Sb_{12} (A=Sr, Ba, La; M=Fe, Ru, Os) used in the band calculations.

Compound	Lattice constant (pm)	u	v
$SrFe_4Sb_{12}$	918.126	0.338393	0.160343
$SrRu_4Sb_{12}$	928.91	0.343316	0.158496
$SrOs_4Sb_{12}$	933.134	0.34154	0.15660
$BaRu_4Sb_{12}$	931.51	0.344393	0.159263
$BaOs_4Sb_{12}$	933.507	0.34174	0.157507
$LaFe_4Sb_{12}$	913.952	0.336966	0.160425

The band-structure calculation was performed using the full potential linearized augmented plane wave plus the local orbital method including spin-orbit coupling implemented in the WIEN2K code.[20] The no overlapping muffin-tin (MT) sphere radii of 2.50, 2.50, and 2.27 bohrs were used for the Sr, Fe, and Sb atoms in $SrFe_4Sb_{12}$, respectively. The radii of all other atoms in other compounds were set to similar values. The value of $R_{MT}K_{max}$ (the smallest MT radius multiplied by the maximum k value in the expansion of plane waves in the basis set), which determines the accuracy of the basis set used, was set to 7.0. The total number of Brillouin zones was sampled with 4000 k points. The lattice constants and positional parameters reported previously[21] for Fe and Ru compounds were used. For Os compounds, the parameters experimentally obtained by x-ray diffraction were used.[22] The lattice constants and the positional parameters for an Sb atom that were used in this paper are listed in Table I.

III. RESULTS AND DISCUSSION

The obtained $R(\omega)$ spectra at 7 and 300 K are shown in Fig. 2. In the figure, the $R(\omega)$ spectrum of $SrFe_4Sb_{12}$ has already reported in the previous paper.[12] The plasma edge ($\hbar\omega_p$) that is the reflectivity minimum in this energy range is located at 0.31 eV in $LaFe_4Sb_{12}$ and at 0.51 eV in $SrFe_4Sb_{12}$. Since $(\hbar\omega_p)^2$ is proportional to the carrier density in the Drude formula, the carrier density of $SrFe_4Sb_{12}$ is higher than that of $LaFe_4Sb_{12}$. The difference in carrier density is due to the different valence numbers of the guest atoms between these materials, specifically, Sr^{2+} in $SrFe_4Sb_{12}$ and La^{3+} in $LaFe_4Sb_{12}$. The increase in carrier density with the decreasing valence number of the guest atoms indicates that positive carriers (holes) are dominant. This is consistent with the band-structure calculations as shown in Fig. 3 and also with the positive value in the thermopower and Hall-coefficient data in the normal state.[14] The band-structure calculations indicate that the overall band structure does not change in these materials, with the E_F of $LaFe_4Sb_{12}$ only shifting by about 30 meV from that of $SrFe_4Sb_{12}$. It was confirmed that in $Na^+Fe_4Sb_{12}$ and $K^+Fe_4Sb_{12}$, $\hbar\omega_p$ is located at 0.6 eV, which is a higher energy than that of $SrFe_4Sb_{12}$.[23] Therefore, the carrier densities of Na and K compounds are higher than that of Sr^{2+} compounds. This indicates that the

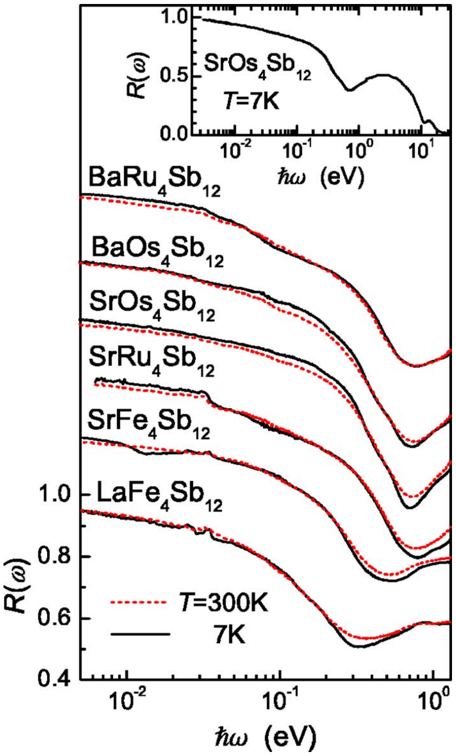

FIG. 2. (Color online) Reflectivity spectra $[R(\omega)]$ of $BaRu_4Sb_{12}$, $BaOs_4Sb_{12}$, $SrOs_4Sb_{12}$, $SrRu_4Sb_{12}$, $SrFe_4Sb_{12}$, and $LaFe_4Sb_{12}$ at 7 (solid lines) and 300 K (dashed lines). Successive curves are offset by 0.2 for clarity. The whole reflectivity spectrum of $SrOs_4Sb_{12}$ in the energy range of 2 meV–30 eV is plotted in the inset.

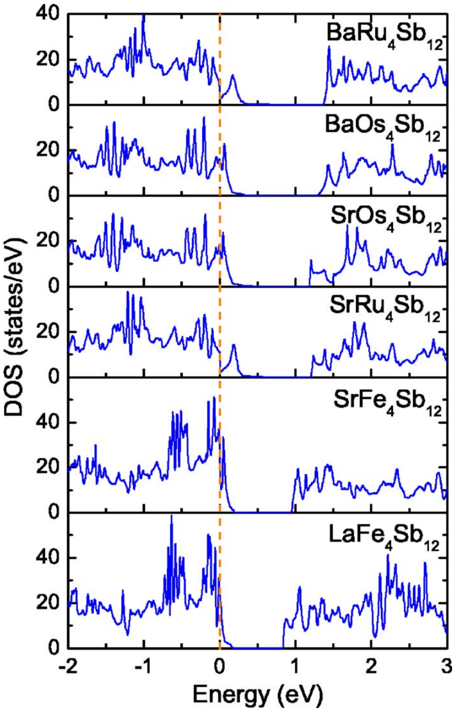

FIG. 3. (Color online) The calculated density of states (DOS) of $LaFe_4Sb_{12}$, $SrFe_4Sb_{12}$, $SrRu_4Sb_{12}$, $SrOs_4Sb_{12}$, $BaOs_4Sb_{12}$, and $BaRu_4Sb_{12}$. The Fermi energy is denoted by a dashed line.

electrons released from the guest atoms control the E_F in the rigid-band-like electronic structure of the Fe_4Sb_{12} cage. It should be noted that in comparing with the band structure among AFe_4Sb_{12} (A=La, Sr, Na) materials, the hybridization band between the Fe $3d$ and Sb $5p$ orbitals commonly exists near the E_F, and that the E_F is determined only by the valence number of the guest atom. This indicates that the $R(\omega)$ minimum not only is the carrier based plasma edge but also includes interband transitions near the E_F, as discussed later. This fine structure near the E_F is smeared out by thermal broadening at 300 K. In this case, the minimum $R(\omega)$ value can be regarded as the carrier plasma edge at 300 K. The spectral weight ($\frac{4m_0}{h^2e^2}\int_0^{\hbar\omega_p}\sigma(\hbar\omega)d\hbar\omega$, where m_0 is the rest mass of an electron and e is the electron charge) below the plasma edge ($\hbar\omega_p$=0.51 eV) of $SrFe_4Sb_{12}$ is evaluated to be 2.7×10^{21} cm^{-3}, which is consistent with the carrier density of $CaFe_4Sb_{12}$ evaluated by the Hall-coefficient measurement.[14]

The next step in this comparison is to make clear which electronic structure an $\sigma(\omega)$ spectrum corresponds to. The $\sigma(\omega)$ spectra at T=7 K and the densities of states (DOSs) above the E_F's of the measured materials are then plotted, as shown in Fig. 4. At 7 K, since the thermal broadening is suppressed, the $\sigma(\omega)$ structure below 0.5 eV can be compared with the band-structure calculation. For $LaFe_4Sb_{12}$, the $\sigma(\omega)$ spectrum monotonically decreases with increasing photon energy for energies less than 0.4 eV with the exceptions of the TO-phonon structure at around 0.02 eV. Above 0.4 eV, the $\sigma(\omega)$ spectrum is dominated by the shoulder structure at around 0.8 eV. The DOS above the E_F also monotonically decreases with increasing energy below 0.15 eV, disappears between 0.2 and 0.8 eV, and appears again above 0.8 eV. In this case, the gaplike structure in the $\sigma(\omega)$ spectrum can be explained by the DOS spectrum above the E_F in which the spectrum is due to the transition from the DOS at the E_F to the unoccupied states.

In the case of $SrFe_4Sb_{12}$, a shoulder structure (unclear, but it is not flat) in the $\sigma(\omega)$ spectrum appears at around $\hbar\omega$ =0.9 eV that corresponds to that at 0.8 eV in $LaFe_4Sb_{12}$. In addition, an additional peak in the $\sigma(\omega)$ appears at 25 meV. Roughly speaking, the additional peak can also be explained by unoccupied states in the DOS, as shown in the inset of Fig. 4. However, the peak in the $\sigma(\omega)$ spectrum is located at 25 meV, while the DOS peak at 50 meV.[24] The origin of this difference is discussed later. Due to the rigid-band-like shift of the E_F, the peak structure that is located below the E_F in $LaFe_4Sb_{12}$ is pushed up above the E_F in $SrFe_4Sb_{12}$. Coincidently, the "V"-shaped DOS peak located 40 meV below the E_F in $LaFe_4Sb_{12}$ is moved up to the E_F. $\sigma(\omega)$ spectra with a narrow pseudogap structure, which commonly appears in $A^{2+}Fe_4Sb_{12}$ materials, reflect the V-shaped DOS of the E_F.[11,12]

In the case of $SrRu_4Sb_{12}$ and $BaRu_4Sb_{12}$, a broad peak in the $\sigma(\omega)$ spectra appears at 0.2 eV that is consistent with the peak in unoccupied states in the DOS, as shown in Fig. 4. In addition, shoulder structures in the $\sigma(\omega)$ spectra appear at 1.25 and 1.35 eV in $SrRu_4Sb_{12}$ and $BaRu_4Sb_{12}$, respectively, that correspond to additional states of the DOS. Based on this analysis, it was concluded that the $\sigma(\omega)$ spectra of

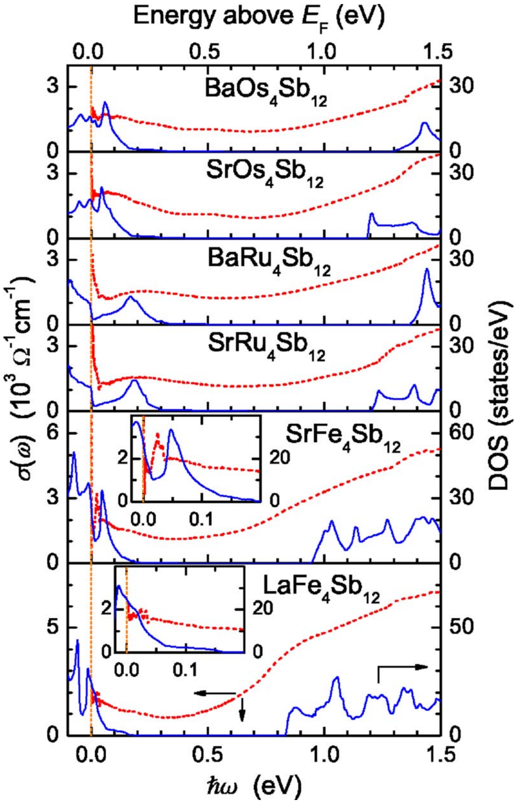

FIG. 4. (Color online) Optical conductivity $[\sigma(\omega)]$ spectra (dashed lines) at T=7 K and the densities of states (DOSs) (solid lines) of BaOs$_4$Sb$_{12}$, SrOs$_4$Sb$_{12}$, BaRu$_4$Sb$_{12}$, SrRu$_4$Sb$_{12}$, SrFe$_4$Sb$_{12}$, and LaFe$_4$Sb$_{12}$. The $\sigma(\omega)$ spectra of Ru and Fe compounds roughly correspond to the unoccupied states in the DOS. The insets in LaFe$_4$Sb$_{12}$ and SrFe$_4$Sb$_{12}$ are a larger scale of each figure below 0.2 eV.

LaFe$_4$Sb$_{12}$, SrFe$_4$Sb$_{12}$, SrRu$_4$Sb$_{12}$, and BaRu$_4$Sb$_{12}$ shown in Fig. 4 correspond to unoccupied states in the DOS.

In the Os compounds, the $\sigma(\omega)$ spectra seem to be explained by these unoccupied states. However, the peak at 0.5 eV of the $\sigma(\omega)$ spectra does not have the corresponding structure in the unoccupied DOS. According to Fig. 3, DOS fine structures exist not only above but also below the E_F for these materials. It is then possible for the occupied states to also determine the $\sigma(\omega)$ spectra. An additional comparison of the calculated $\sigma(\omega)$ spectra from the band-structure calculations to the experimental $\sigma(\omega)$ spectra is then required.

To clarify the effect of the different atoms in Fe, Ru, and Os to the electronic structure in detail, the experimental $\sigma(\omega)$ spectra are compared with the theoretical ones obtained from the band-structure calculation. The $\sigma(\omega)$ spectra due to interband transitions are derived from the function as follow in which the direct transition is assumed:[25]

$$\sigma(\omega) = \frac{\pi e^2}{m_0^2 \omega} \sum_{\vec{k}} \sum_{nn'} \frac{|\langle n'\vec{k}|\vec{e}\cdot\vec{p}|n\vec{k}\rangle|^2}{\omega - \omega_{nn'}(\vec{k}) + i\Gamma} \times \frac{f(\epsilon_{n\vec{k}}) - f(\epsilon_{n'\vec{k}})}{\omega_{nn'}(\vec{k})}.$$

Here, the $|n'\vec{k}\rangle$ and $|n\vec{k}\rangle$ states denote the occupied and unoccupied states, respectively, $f(\epsilon_{n\vec{k}})$ is the Fermi-Dirac function, $\hbar\omega_{nn'} = \epsilon_{n\vec{k}} - \epsilon_{n'\vec{k}}$ is the energy difference of the unoccupied and occupied states, and Γ is the lifetime parameter. In the calculation, Γ=1 meV was assumed.

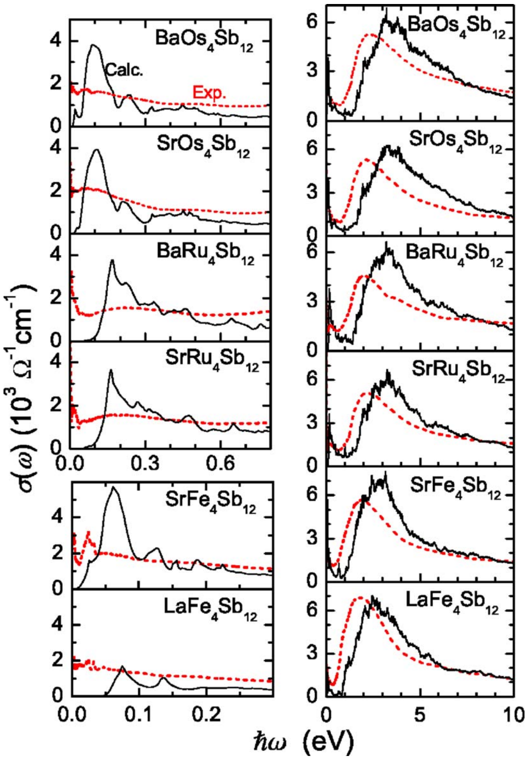

FIG. 5. (Color online) Experimental optical conductivity $[\sigma(\omega)]$ spectra (dashed lines) compared with the corresponding calculated ones (solid lines) of AM_4Sb$_{12}$ (A=Ba, Sr, La; M=Fe, Ru, Os). The left figures are expansions of the low-energy region. The $\sigma(\omega)$ spectra in the left and right figures were taken at 7 and 300 K, respectively.

The calculated and the corresponding experimental $\sigma(\omega)$ spectra of all materials are shown in Fig. 5. The experimental spectra over the wide energy range in the right figures of Fig. 5 have a tail toward the higher-energy side, which was reproduced by the calculation with reasonable accuracy. However, the large peak experimentally observed at around $\hbar\omega$ =2 eV that corresponds to the interband transition from the valence to conduction bands is located at about 3 eV in the calculated spectra. The experimental peak slightly shifts to the higher-energy side changing from M=Fe to Os, and the corresponding peak in LaFe$_4$Sb$_{12}$ is located at a lower energy than that of SrFe$_4$Sb$_{12}$. The shifts in the peak energies are consistent with the calculations. By comparison, the spectral features in the lower-energy region shown in the left figures in Fig. 5 drastically change with changing M. In the case of SrFe$_4$Sb$_{12}$, as reported in previous papers,[11,24] a pseudogap appears below 14 meV, and a peak is present at around 25 meV. In comparing the calculated spectra with LaFe$_4$Sb$_{12}$, the $\sigma(\omega)$ spectrum of SrFe$_4$Sb$_{12}$ has a peak at 60 meV. This peak was assumed to correspond to the experimental peak at 25 meV despite the large energy difference. The origin of this inconsistency is discussed later.

In the case of Ru compounds, a broad peak was experimentally observed at 0.2 eV. There is a corresponding peak at the same energy in the calculated spectrum. In the case of

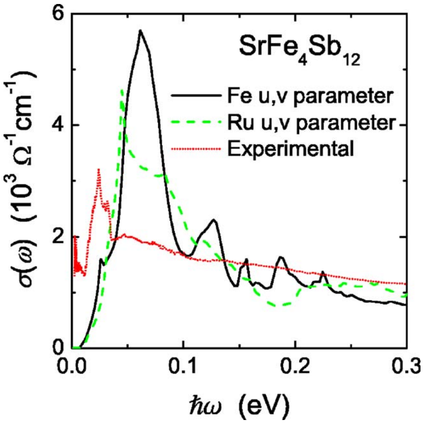

FIG. 6. (Color online) Calculated optical conductivity $[\sigma(\omega)]$ spectra of $SrFe_4Sb_{12}$ using the positional parameters of $SrFe_4Sb_{12}$ (solid line) and of $SrRu_4Sb_{12}$ (dashed line) compared with the experimental spectrum (dotted line).

Os compounds, two peaks at 0.1 and 0.5 eV and a shoulder at 0.22 eV were experimentally observed. All of these structures were reproduced by the calculation. Based on this, all of the experimental $\sigma(\omega)$ spectra of the AM_4Sb_{12} materials reported here can be qualitatively reproduced by the band calculation. In comparison with the other experiments, the order of the peak energies for M is the same as for the other physical properties of these materials. For instance, the electronic specific-heat coefficient γ is 100, 10, and 45 mJ/mol K^2 in M=Fe, Ru, and Os, respectively. This indicates that the low-energy peak in the $\sigma(\omega)$ spectra as well as the shape of the DOS near the E_F strongly affect the thermodynamical physical properties in AM_4Sb_{12} materials.

The possibilities of the origin of the difference of the spectral shapes among M=Fe, Ru, Os in the infrared region include the different positional parameters of Sb ions and the differences in the wave function of the d electrons due to the different principal quantum numbers of M atoms. In order to ascertain the effects of the different positional parameters, the $\sigma(\omega)$ spectrum of $SrFe_4Sb_{12}$ with the positional parameter of the Ru counterpart was calculated, as shown in Fig. 6. The characteristic peak at 60 meV is again present even using the Ru positional parameters, although the intensity is lower. This result indicates that the positional parameters of Sb ions do not affect the electronic structure near the E_F, but the differences in the wave functions of the d states in M =Fe, Ru, Os are dominant. Therefore, the differences in the physical properties among these materials are also due to the different wave functions of the d states. Particularly in the case of $SrFe_4Sb_{12}$, the electronic structure near the E_F is largely determined by the Fe 3d–Sb 5p hybridization state. The pseudogap structure as well as the narrow peak structure at 25 meV are concluded to originate from the localization of the Fe 3d state. As noted previously, the experimentally obtained peak energy of 25 meV for $SrRu_4Sb_{12}$ is lower than the calculated one (60 meV), which is not the case for the other compounds. This low-energy shift in the experimental peak might be due to the renormalization effect arising from the strong electron correlation or due to the self-energy effect observed in the photoemission spectra.[26] The existence of heavy quasiparticles originating from the Fe 3d state has already been reported.[12] The origin of the heavy quasiparticles is believed to be the Kondo effect resulting from the hybridization between the localized Fe 3d state and conduction band. However, since $SrFe_4Sb_{12}$ is located very near the ferromagnetic ordering state, the spin fluctuation effect must also be considered. Heavy quasiparticles due to the spin fluctuation are also predicted by the SCR theory.[27,28] Both the peak shift and the presence of heavy quasiparticles suggest that the Fe 3d state in $SrFe_4Sb_{12}$ has stronger electron correlation than the Ru and Os compounds.

IV. CONCLUSION

In summary, to investigate the electronic structure of the M_4Sb_{12} cage in AM_4Sb_{12} (A=Sr, Ba, La; M=Fe, Ru, Os) materials, we measured the optical conductivity $[\sigma(\omega)]$ spectra and compared with band-structure calculations as well as calculated $\sigma(\omega)$ spectra. Both the energy shift of the plasma edge due to the different valence number of guest atoms A in the Fe_4Sb_{12} cage and the corresponding band calculation suggest the hole-type carriers. The experimental $\sigma(\omega)$ spectra were reasonably well reproduced by the band calculations using experimental lattice constants and positional parameters. The $\sigma(\omega)$ spectra of SrM_4Sb_{12} (M=Fe, Ru, Os) in the infrared region drastically change with different M. This change does not originate from the different positional parameters of Sb ions but from the different wave functions of d states due to the different principal quantum numbers of M ions.

ACKNOWLEDGMENTS

We would like to thank K. Takegahara for the fruitful discussion and suggestions. This work was a joint studies program of the Institute for Molecular Science (2005) and was partially supported by a Grant-in-Aid, the COE Research (Grant No. 13CE2002), the priority area "Skutterudite" (No. 15072205), and Scientific Research (B) (No. 18340110) from MEXT of Japan.

---

*Electronic address: kimura@ims.ac.jp

†Present address: Department of Physics, Sungkyunkwan University, Korea.

‡Present address: Department of Physics, Tohoku University, Sendai, Japan.

[1] Y. Aoki, A. Tsuchiya, T. Kanayama, S. R. Saha, H. Sugawara, H. Sato, W. Higemoto, A. Koda, K. Ohishi, K. Nishiyama, and R. Kadono, Phys. Rev. Lett. **91**, 067003 (2003).

[2] A. Miyake, K. Shimizu, C. Sekine, K. Kihou, and I. Shirotani, J. Phys. Soc. Jpn. **73**, 2370 (2004).

[3] T. Tayama, J. Custers, H. Sato, T. Sakakibara, H. Sugawara, and H. Sato, J. Phys. Soc. Jpn. **73**, 3258 (2004).

[4] K. Hachitani, H. Fukazawa, Y. Kohori, I. Watanabe, C. Sekine, and I. Shirotani, Phys. Rev. B **73**, 052408 (2006).

[5] H. Sato, H. Sugawara, D. Kikuchi, S. Sanada, K. Tanaka, H. Aoki, K. Kuwahara, Y. Aoki, and M. Kohgi, Physica B **378-380**, 46 (2006).

[6] K. Takegahara, H. Harima, and A. Yanase, J. Phys. Soc. Jpn. **70**, 1190 (2001); **70**, 3468 (2001); **71**, 372 (2002).

[7] H. Harima and K. Takegahara, J. Phys.: Condens. Matter **15**, S2081 (2003).

[8] A. Leithe-Jasper, W. Schnelle, H. Rosner, N. Senthilkumaran, A. Rabis, M. Baenitz, A. Gippius, E. Morozova, J. A. Mydosh, and Y. Grin, Phys. Rev. Lett. **91**, 037208 (2003).

[9] A. Leithe-Jasper, W. Schnelle, H. Rosner, M. Baenitz, A. Rabis, A. A. Gippius, E. N. Morozova, H. Borrmann, U. Burkhardt, R. Ramlau, U. Schwarz, J. A. Mydosh, Y. Grin, V. Ksenofontov, and S. Reiman, Phys. Rev. B **70**, 214418 (2004).

[10] G. Sheet, H. Rosner, S. Wirth, A. Leithe-Jasper, W. Schnelle, U. Burkhardt, J. A. Mydosh, P. Raychaudhuri, and Yu. Grin, Phys. Rev. B **72**, 180407(R) (2005).

[11] J. Sichelschmidt, V. Voevodin, H. J. Im, S. Kimura, H. Rosner, A. Leithe-Jasper, W. Schnelle, U. Burkhardt, J. A. Mydosh, Yu. Grin, and F. Steglich, Phys. Rev. Lett. **96**, 037406 (2006).

[12] S. Kimura, T. Mizuno, H. J. Im, K. Hayashi, E. Matsuoka, and T. Takabatake, Phys. Rev. B **73**, 214416 (2006).

[13] K. Koga, K. Akai, K. Oshiro, and M. Matsuura, Phys. Rev. B **71**, 155119 (2005).

[14] T. Takabatake, E. Matsuoka, S. Narazu, K. Hayashi, S. Morimoto, T. Sasakawa, K. Umeo, and M. Sera, Physica B **383**, 93 (2006).

[15] E. Matsuoka, K. Hayashi, A. Ikeda, K. Tanaka, T. Takabatake, and M. Matsumura, J. Phys. Soc. Jpn. **74**, 1382 (2005).

[16] M. Matsumura, G. Hyoudou, H. Kato, T. Nishioka, E. Matsuoka, H. Tou, T. Takabatake, and M. Sera, J. Phys. Soc. Jpn. **74**, 2205 (2005).

[17] E. Matsuoka, S. Narazu, K. Hayashi, K. Umeo, and T. Takabatake, J. Phys. Soc. Jpn. **75**, 014602 (2006).

[18] K. Fukui, H. Miura, H. Nakagawa, I. Shimoyama, K. Nakagawa, H. Okamura, T. Nanba, M. Hasumoto, and T. Kinoshita, Nucl. Instrum. Methods Phys. Res. A **467-468**, 601 (2001).

[19] M. Dressel and G. Grüner, *Electrodynamics of Solids* (Cambridge University Press, Cambridge, 2002).

[20] P. Blaha, K. Schwarz, G. K. H. Madsen, D. Kvasnicka, and J. Luitz, WIEN2K, Vienna University of Technology, 2001, improved and updated Unix version of the original copyrighted WIEN code, which was presented by P. Blaha, K. Schwarz, P. Sorantin, and S. B. Trickey, Comput. Phys. Commun. **59**, 339 (1990); http://www.wien2k.at

[21] J. W. Kaiser and W. Jeitschko, J. Alloys Compd. **291**, 66 (1999).

[22] M. Tsubota (private communication).

[23] J. Sichelschmidt *et al.*, report (unpublished).

[24] S. Kimura, H. J. Im, Y. Sakurai, T. Mizuno, K. Takegahara, H. Harima, K. Hayashi, E. Matsuoka, and T. Takabatake, Physica B **383**, 137 (2006).

[25] V. Antonov, B. Harmon, and A. Yaresko, *Electronic Structure and Magneto-Optical Properties of Solids* (Kluwer Academic, Dordrecht, 2004).

[26] A. A. Kordyuk, S. V. Borisenko, A. Koitzsch, J. Fink, M. Knupfer, and H. Berger, Phys. Rev. B **71**, 214513 (2005).

[27] H. Hasegawa, J. Phys. Soc. Jpn. **46**, 831 (1979).

[28] T. Moriya and Y. Takahashi, J. Phys. Soc. Jpn. **60**, 776 (1991).